

## Numerical Simulation of Ice-breaking Process of Rigid Structure Based on Peridynamics Method

Yifan Li<sup>1</sup>, Guohua Pan<sup>2</sup>, Fengze Xie<sup>1</sup>, Decheng Wan<sup>1\*</sup>

<sup>1</sup> Computational Marine Hydrodynamics Lab (CMHL), School of Naval Architecture, Ocean and Civil Engineering,  
Shanghai Jiao Tong University, Shanghai, China

<sup>2</sup> Ningbo Pilot Station, Ningbo Dagang Pilotage Co., Ltd., Ningbo, China

\*Corresponding author

### ABSTRACT

As a heavy weapon of great powers, submarines play an important role in the strategic competition in the polar region. The existence of ice sheet in the polar region has an impact on the navigation of submarines, especially hindering their surfacing movement. The bond-based peridynamics (BBPD) method is used to simulate the ice-breaking process of submarine surfacing. The accuracy of the numerical model is verified by the four-point bending of columnar ice. The numerical ice-breaking model is simplified to the interaction between the structure and an ice sheet. During the ice-breaking process of the structure, the formation and evolution process of ice fractures is concerned as well as the time history of load on the structure is recorded.

**KEY WORDS:** Peidynamics (PD); ice-structure interaction; ice failure process; ice load.

### INTRODUCTION

With the increase in global resource demand, the value of channel development and resource development in polar regions has gradually become prominent. In polar engineering, it is of great application value to break ice through rigid structures. Under the impact of structure, the dynamic fracture mechanism of ice is very complicated. It is very important to study the fracture behavior of ice under impact conditions to reveal its material properties and failure mechanism. It can not only provide valuable reference for polar engineering but also has practical significance for the exploration of polar resources and the development of equipment and technology.

At present, many methods have been applied to the numerical simulation of ice-structure interaction at home and abroad. The finite element method (FEM) is widely used to evaluate the fracture behavior and load characteristics of ice sheets. Kim et al. (2013 & 2014) used the FEM model to numerically study the resistance performance of icebreakers under floating ice conditions. The accuracy of the numerical model was verified by comparing the experimental results.

Based on this model, the resistance performance of icebreakers at different waterline angles was studied. Although the FEM method can simulate the fracture process of ice, its assumption based on continuity does not apply to the discontinuous displacement field at ice fractures, which poses a challenge in solving complex dynamic discontinuities, especially for predicting the dynamic propagation path of fractures and revealing the mechanism of ice failure.

The meshless method has gradually emerged in the study of ice structure interaction, such as the discrete element method (DEM). Ji et al. (2016) established the three-dimensional DEM with bonded-particles to simulate the failure process of sea ice. Through the DEM simulation of the uniaxial compressive and flexural strength of sea ice, the influence of the friction coefficient between particles and the bonding strength of the bonded particles on the failure process of sea ice were analyzed. According to the numerical simulation results, the relationship between interparticle strength and macrostrength are determined. Long et al. (2020) applied the DEM model to simulate the ice failure mode and ice load during the interaction between sea ice and conical structure. The effects of ice thickness, ice velocity, cone diameter and cone angle on ice breaking length and ice load are considered in the simulation. Finally, the calculation formula of ice load considering the influence of ice breaking length is proposed. DEM has advantages in simulating the discontinuous stage of the fracture process, but the accuracy of the continuous stage makes it possible to make mistakes in simulating the whole process from continuous to discontinuous.

Proposed by Silling (2000), Peridynamics (PD) method is a nonlocal continuum solid mechanics method, which has the characteristics of a meshless method. Different from the partial differential equations commonly used in traditional mesh-based methods, the equation of motion in the PD method is defined in the integral form, so it is applicable to solve discontinuous problems. PD can spontaneously simulate the generation and propagation of fractures without presetting, making it well-suited for solving material damage and fracture problems such as fracture formation and extension processes. Based on the bond-based PD (BBPD) method, Wang et al. (2018) established a

constitutive model to characterize the elastic-brittle mechanical properties of ice at high strain rates to study the crushing effect of underwater explosion load on the ice sheet. The formation and propagation of fractures in the damage process were simulated, which agreed well with the experimental results. Focusing on the process of propeller-ice, Xiong et al. (2020) applied a PD numerical model to study the influence mechanism of shadow effect on sea ice failure mode and the load acting on the propeller. Additionally, a new analytical shadowing effect coefficient on the ratio of the front and back contacts divided by the axial length of the damaged ice is proposed. Zhang et al. (2023) conducted a numerical simulation of the high-speed impact of rigid balls on the ice sheet based on the BBPD method. According to different impact velocities, ice thicknesses and boundary constraints, the detailed fracture characteristics that were not observed in the experiment were well demonstrated in the numerical simulation. The above research proves that the PD method is suitable for a wide range of problems and the simulation effect is ideal.

In this paper, the BBPD method is used to establish the numerical model of the interaction between ice and structure. The accuracy of the numerical model is verified based on the four-point bending experiment (Ehlers and Kujala, 2014). Based on the above validation, the numerical simulation of the ice-breaking process of a cylindrical penetrating ice sheet and submarine surfacing is carried out. In the simulation, the characteristics of ice fractures and the variation of ice load are focused on.

## NUMERICAL METHOD

### Motion Equations and Constitutive Relation

The discrete PD can be regarded as macroscopic molecular dynamics in a continuous state. The core idea of PD is to discretize the research target into a series of material points. The interaction between these material points is not limited to directly adjacent points. In the theory of BBPD, at time  $t$ , the motion equation of any material point with position  $x$  in the reference configuration (shown in Fig.1) can be written as follows:

$$\rho \ddot{u}(x, t) = \int_{H_x} f(u(x', t) - u(x, t), x' - x) dV_{x'} + b(x, t) \quad (1)$$

where  $\rho$  is the material density;  $\ddot{u}$  is the acceleration vector;  $H_x$  is the collection of other material points within the horizon range of the material point  $x$ , i.e.  $H_x = \{x' \in R : \|x' - x\| < \delta\}$ ,  $\delta$  is the radius of the horizon;  $f$  is the interaction force density of the material points  $x$  and  $x'$  at time  $t$ ;  $u$  is the displacement vector;  $V_{x'}$  is the volume of the material point  $x'$ ;  $b$  is the body force density.

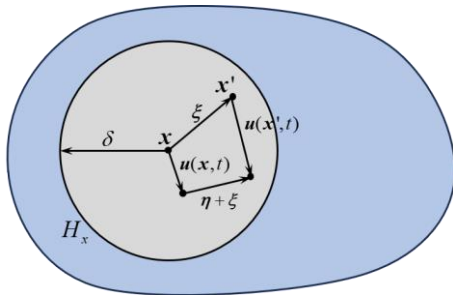


Fig. 1 Interaction between material points with the horizon

In the horizon range,  $\xi = x' - x$  is defined as the relative position of the material points  $x$  and  $x'$ , as well as  $\eta = u(x', t) - u(x, t)$  is defined as the relative position of the above pair of material point at time  $t$ . In this study, the prototype microelastic brittle (PMB) model proposed by Silling et al. (2005) is used to describe the constitutive relationship of ice sheet. It is isotropic in the initial state. In the theory of BBPD, the pairwise force function between material point pairs can be expressed as follows:

$$f(\eta, \xi) = \frac{\partial \omega(\eta, \xi)}{\partial \eta} = cs \frac{\eta + \xi}{|\eta + \xi|} \mu(t, \xi) \quad (2)$$

where  $\omega(\eta, \xi)$  is the microscopic elastic strain energy density of the bonds, which is a scalar function;  $c$  is the microelastic modulus of the material, which represents the elastic stiffness of the bonds;  $s$  is the bond stretch between the material points at any time  $t$ ;  $\mu(t, \xi)$  will be introduced in the next section. The expressions of  $\omega(\eta, \xi)$  and  $s$  are as follows:

$$\omega(\eta, \xi) = \frac{cs^2}{2} |\xi| \quad (3)$$

$$s = \frac{|\eta + \xi| - |\xi|}{|\xi|} \quad (4)$$

The energy density of the volume contained in the target material point within the horizon range should be equal to the strain energy density in the classical theory of elasticity for the same material and the same deformation (Silling et al., 2005). Therefore, the elastic stiffness of the ice sheet can be written as follows:

$$c = \frac{18k}{\pi\delta^4} = \frac{6E}{\pi\delta^4(1-2\nu)} \quad (5)$$

where  $k$  is the bulk modulus;  $E$  is the elastic modulus;  $\nu$  is the Poisson's ratio, which is 1/4 in the three-dimensional simulation. When PD is used to simulate the impact damage problem, Poisson's ratio has little effect on the fracture propagation speed and path (Silling et al., 2007). Therefore, Poisson's effect is not discussed in this study.

### Failure Model of Ice Sheet

In order to describe the ice fracture phenomenon under the impact of the structure, the following time-dependent breaking criterion function needs to be introduced:

$$\mu(t, \xi) = \begin{cases} 1 & \text{if } s(t', \xi) < s_0 \text{ for all } 0 \leq t' \leq t, \\ 0 & \text{otherwise.} \end{cases} \quad (6)$$

where  $s_0$  is the critical stretch for bond failure, which means that when the bond between any two material points is stretched to exceed a certain critical value, the bond connecting the two material points will break and fail, and there is no force between the material points. This failure will not change over time. For the ice sheet used in this study, the critical stretch  $s_0$  is expressed as follows:

$$s_0 = \sqrt{\frac{10G_0}{\pi c \delta^5}} = \sqrt{\frac{5G_0}{9k\delta}} \quad (7)$$

where  $G_0$  is the critical energy release rate of the material, also known as fracture energy.

Although the ice sheet in this study is isotropic in the initial state, the bond failure in a certain direction will lead to the anisotropy of the subsequent response. Here, a damage index is introduced to describe the damage degree of the material point:

$$\varphi(\mathbf{x}, t) = 1 - \frac{\int_{H_x} \mu(\mathbf{x}, t, \xi) dV_\xi}{\int_{H_x} dV_\xi} \quad (8)$$

where  $\varphi \in [0, 1]$ . When  $\varphi = 1$ , the bonds between all the material points within the horizon of target material point are all of failure; when  $\varphi = 0$ , the material is in the initial state, the bonds between the material points do not fail. It is not difficult to see that the damage index indicates the degree of damage of the material point within a certain time range, that is, the ratio of the bond failure to all the bonds in the horizon range of the target material point.

## RESULTS AND DISCUSSIONS

### Validation of Numerical Model

#### Numerical model

To demonstrate the accuracy of the present numerical model, we used the BBPD method to simulate the failure process of columnar ice in the four-point bending test. In this section, the convergence analysis is carried out by simulating three models with different particle spacing. The numerical results are compared with the experimental measurement of Ehlers and Kujala (2013).

The size settings in the experiment are used to establish the numerical model of four-point bending, which consists of three parts, namely, the columnar ice, the upper and the lower supports. The length, width and height of columnar ice are 4.32 m, 0.36 m and 0.39 m. The upper and lower supports are regarded as rigid bodies, which are 2 m and 0.5 m away from the ice center, respectively. The two lower supports move upward at a speed of 0.003 m/s. The material parameters of ice are set as shown in Table 1. The three particle spacings are  $dx=0.015$  m,  $dx=0.02$  m and  $dx=0.025$  m, while the radius of the horizon  $\delta = 4dx$ . The time step is set to  $5.0 \times 10^{-5}$  s.

Table 1. Parameters of ice material

Young's Modulus	Density	Critical Stretch	Poisson's Ratio
5.0 GPa	900 kg/m <sup>3</sup>	0.0015	0.25

#### Comparison of numerical and experimental results

In the numerical simulation, due to the upward movement of the lower supports, the columnar ice presents a state where the bottom is compressed and the top is stretched. Finally, fractures are first generated on the upper surface. The fracture forms a cross-section in a very short period, which means the ice failure. The comparison of the ice failure in the four-point bending test obtained by the simulations of PD and SPH (Das et al., 2014) is shown in Fig.2. Two simulation results are in good agreement, while more detailed descriptions of the damage degree are shown in the PD result.

As shown in Fig.3, the time history curves of bending force obtained by the PD numerical models with different particle spacing agree well with the experimental result. With the decrease of particle spacing, the early oscillation of the curve is alleviated. The maximum force with corresponding time in numerical simulations of different particle spacing and experimental results are presented in Table 2. Considering both the accuracy and efficiency of computation, particle spacing of  $dx=0.02$  m is suitable for simulation.

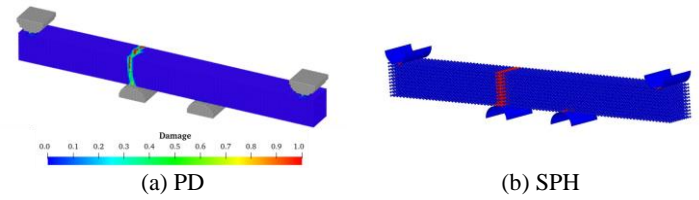


Fig.2 Comparison of ice failure by two numerical methods

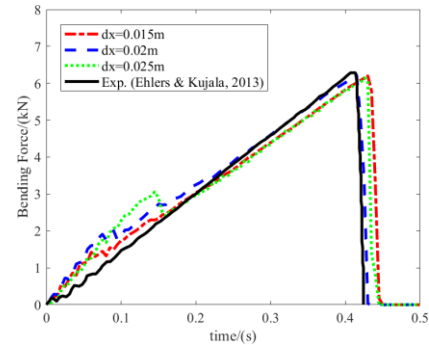


Fig.3 Comparison of PD results and experiment

Table 2 Comparison of maximum force in PD and experimental results

Case	Maximum Force	Corresponding Time
$dx=0.015$ m	6.201 kN	0.430 s
$dx=0.02$ m	6.226 kN	0.415 s
$dx=0.025$ m	6.152 kN	0.425 s
Exp.	6.286 kN	0.413 s

### Simulation of a Cylinder Penetrating Ice Sheet

For further study of the interaction between ice and structure, the simulation of the vertical upward movement of a cylinder penetrating ice sheet is carried out in this section. The schematic graph of the initial numerical model is shown in Fig.4. The length, width and thickness of the ice sheet are  $L=4$  m,  $W=4$  m and  $H=0.1$  m, respectively. The material of the ice sheet is the same as in Table 1. The diameter of the cylinder is 0.2 m. At a constant velocity of  $v=0.1$  m/s, the cylinder moves upwards below the center of the ice sheet. In this process, the cylinder is regarded as a rigid body, and the edge of the ice sheet is fixed. The particle spacing, radius of horizon and time step are the same as validation.

As is shown in Fig.5, the PD simulation results of the fracture propagation on the ice sheet are compared with the sketch obtained by the experimental observation (Ashton, 1986). The time instants given in Fig.5 are limited to the description of numerical simulation, which are  $t=0.08$  s,  $t=0.26$  s,  $t=0.40$  s and  $t=0.90$  s, respectively. From the law of fracture propagation, radial fractures occur earlier than circumferential fractures. With the upward motion of the cylinder, the number of radial

fractures gradually develops from 2 to 4, and then to 8, corresponding to (a), (b) and (c) in Fig.5. When the circumferential fracture is generated, it also means the failure of the ice sheet, and the ice sheet produces obvious conical damage, corresponding to (d) in Fig.5. The time history curve of vertical ice load force is shown in Fig.6. During the first half of the cylinder upward movement, the ice load increases slowly, and the length and number of radial fractures develop. At about  $t=0.40$  s, the ice load reaches the maximum value, while eight radial fractures are formed in the ice sheet. At about  $t=0.9$  s, the circumferential fracture occurs, the ice load decreases sharply in a short time, and finally tends to zero, which also means the failure of the ice sheet.

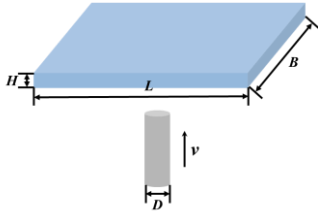


Fig.4 Schematic graph of cylinder moving upward

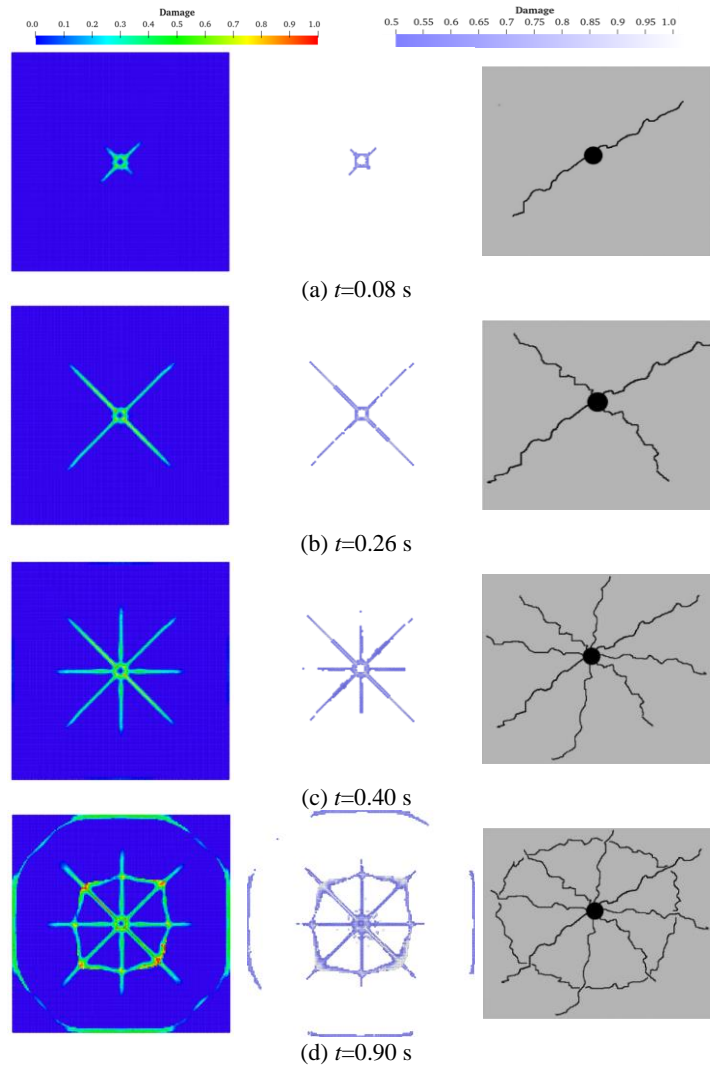


Fig.5 Comparison of numerical results (at typical instants) and sketch from experimental observation

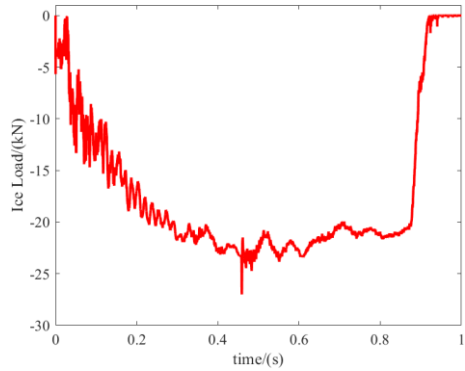


Fig.6 Time history of the vertical ice load during cylinder moving upward

### Simulation of ice-breaking process of submarine surfacing

After the above simulations of the simple model, the feasibility of the PD model used in this paper has been verified. In this section, the PD model will be used to simulate the ice-breaking process of submarine surfacing, focusing on the characteristics of ice fractures and the law of ice load. The target numerical model (shown in Fig.7) will be simplified as the interaction between the structure and the ice sheet. The length, width and thickness of the ice sheet are  $L=6$  m,  $W=1.5$  m and  $H=0.02$  m, respectively. The submarine in simulation is carried out on the model-scale model of SUBOFF, whose main parameters are presented in Table 3. The surfacing velocity of the submarine is set to  $v=0.25$  m/s. The treatment of the structure and the ice sheet boundary is the same as in the previous section.

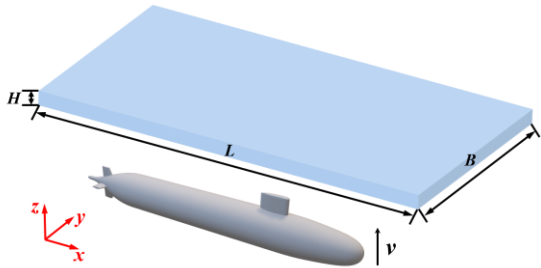


Fig.7 Schematic graph of submarine surfacing process

Table 3 Main parameters of SUBOFF with model scale

Parameters	Values
Overall length	4.356 m
Maximum diameter of hull	0.508 m
Maximum height	0.734 m
Length of conning tower	0.368 m

As is shown in Fig.8 (a), in the whole ice-breaking process, the conning tower first contacts with the ice sheet, resulting in a fracture similar to its contour shape. In this process, the hull will not contact with the ice sheet, so the damage of the ice sheet presents local characteristics, which are shown in Fig.8 (b) and (c). With the upward motion of the submarine, the top of the hull begins to contact with the ice sheet. As shown in Fig.8 (d), a slender fracture along the direction of the hull is

generated. As shown in Fig.8 (e), the contact between the tail fin and the ice sheet will produce crossed radial fractures, which will accelerate the failure of the ice sheet. Finally, the ice sheet is lifted upward, resulting in overall fractures, which is shown in Fig.8 (f).

The time history of ice load during the surfacing process is shown in Fig.9. Only the load in z direction is shown since the ice load in x and y directions is too small compared to the load in z direction. The moment  $t=0$  s is defined as the time when the conning tower contacts the ice sheet causing damage. The damage of the ice sheet can be roughly divided into three stages. In the first stage, the damage is mainly caused by the impact of the conning tower on the ice sheet, while the first load peak value appears in the early period. After the first stage, a completely broken ice block is formed at the top of the conning tower. During the period of the conning tower penetrating the ice sheet, i.e. the second stage, there is no direct contact between the structure and the ice sheet in the vertical direction, leading to the ice load approaching zero. In the third stage, the load reaches the second peak, and the ice sheet produces a larger-scale fracture due to the contact of the upper hull. Finally, the ice load tends to zero again, which means the failure of the ice sheet.

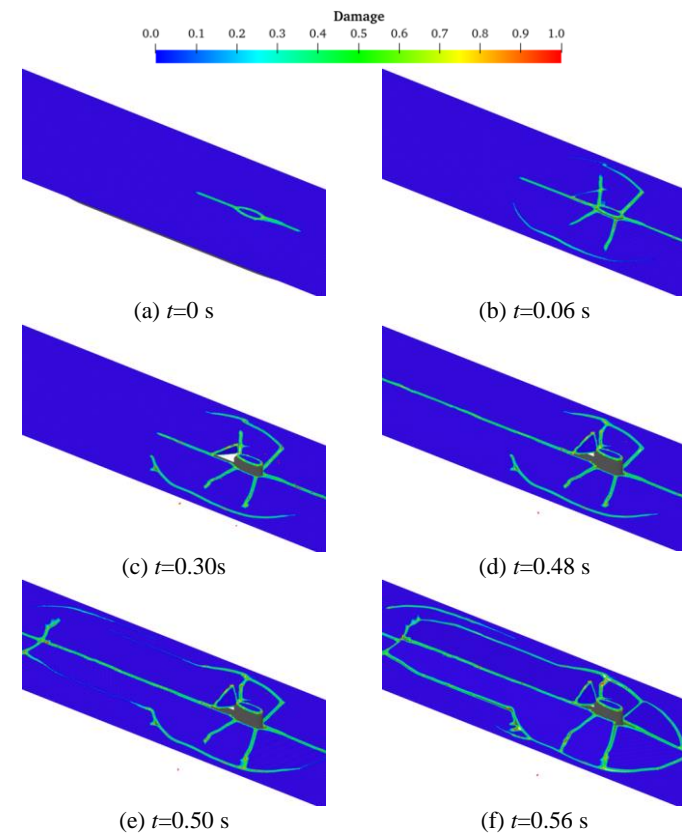


Fig.8 Schematic graph of submarine surfacing process obtained by numerical simulation

## CONCLUSIONS

In this paper, a numerical solution of the PD method is given for the problem of interaction between rigid structures and the ordinary ice sheet. Combined with the theoretical research of the PD method, a three-dimensional PD numerical model for simulating the damage degree of ice is established in the corresponding problem. Through comparison with the experimental results, the accuracy of the numerical

model based on the PD method is validated. Based on the above validation, the numerical simulations of the ice-breaking process of the cylinder penetrating the ice sheet and the submarine surfacing are carried out, focusing on the characteristics of fracture and the law of ice load under the dynamic motion of the structure. The following main conclusions can be drawn:

In the simulation of the four-point experiment of columnar ice, the time history curves of bending force agree well with the experiment in the simulations of different particle spacing, and the ice fracture is similar to the SPH result.

In the simulation of a cylinder penetrating ice sheet, the occurrence of radial fractures is earlier than that of circumferential fractures. The number of radial fractures increases first, while the occurrence of the circumferential fractures means the failure of ice sheet. The damage degree of the ice and the development of the fracture can be captured. The characteristics of fractures are in good agreement with the experimental observation.

The interaction between the structure and the ice sheet during the process of the ice-breaking process of submarine surfacing is vividly depicted by numerical simulation. Local fractures are generated by the upward movement of the conning tower, while the overall failure of the ice sheet occurs after the impact of the upper hull. Through the analysis of the time history of ice load, the ice-breaking process is divided into three stages. The peak load appears in the first and third stages, which are due to the impact of the conning tower and the hull, respectively. In the second stage, the load is close to zero since the submarine has almost no contact with the ice sheet.

This study helps understand the damage process of ice and the variation of ice load in the interaction between ice and structure, which lays a good foundation for the future study of complex ice-water-structure coupling problems.

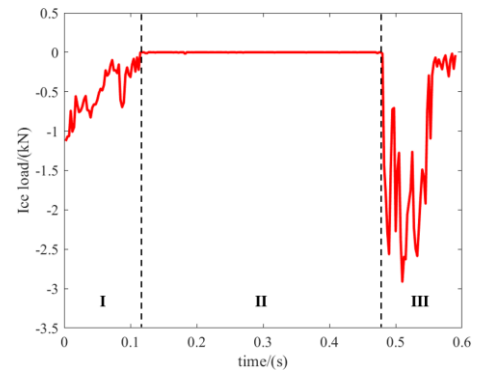


Fig.9 Time history of ice load during the surfacing process

## ACKNOWLEDGEMENT

This work is supported by the National Natural Science Foundation of China (52131102), to which the authors are most grateful.

## REFERENCES

- Ashton G D (1986). "River and lake ice engineering," *Water Resources Publication*.
- Das J, Polić D, Ehlers S, et al. (2014). "Numerical simulation of an ice

- beam in four-point bending using SPH,” *Int Conf on Offshore Mech and Arctic Eng.* ASME, 45561: V010T07A013.
- Ehlers S and Kujala P (2014). “Optimization-based material parameter identification for the numerical simulation of sea ice in four-point bending,” *Proc. IME M: J Eng Marit Environ*, 228(1), 70–80.
- Ji S, Di S and Long X (2017). “DEM simulation of uniaxial compressive and flexural strength of sea ice: parametric study,” *J Eng Mech*, 143(1): C4016010.
- Kim M C, Lee S K, Lee W J, et al. (2013). “Numerical and experimental investigation of the resistance performance of an icebreaking cargo vessel in pack ice conditions,” *Int J Nav Arch Ocean*, 5(1): 116-131.
- Kim M C, Lee W J and Shin Y J (2014). “Comparative study on the resistance performance of an icebreaking cargo vessel according to the variation of waterline angles in pack ice conditions,” *Int J Nav Arch Ocean*, 6(4): 876-893.
- Long X, Liu S and Ji S (2020). “Discrete element modelling of relationship between ice breaking length and ice load on conical structure,” *Ocean Eng*, 201: 107152.
- Silling S A (2000). “Reformulation of elasticity theory for discontinuities and long-range forces,” *J Mech Phys Solids*, 48(1): 175-209.
- Silling S A and Askari E (2005). “A meshfree method based on the peridynamic model of solid mechanics,” *Comput Struct*, 83(17-18): 1526-1535.
- Silling S A, Epton M, Weckner O, et al (2007). “Peridynamic states and constitutive modeling,” *J elasticity*, 88: 151-184.
- Wang Q, Wang Y, Zan Y, et al (2018). “Peridynamics simulation of the fragmentation of ice cover by blast loads of an underwater explosion,” *J Mar Sci Tech*, 23: 52-66.
- Xiong W P, Wang C, Wang C H, et al (2020). “Analysis of shadowing effect of propeller-ice milling conditions with peridynamics,” *Ocean Eng*, 195: 106591.
- Zhang Y, Wang Q, Oterkus S, et al (2023). “Numerical investigation of ice plate fractures upon rigid ball impact,” *Ocean Eng*, 287: 115824.